SPARSE MULTIPATH WIRELESS CHANNELS: MODELING AND IMPLICATIONS

Akbar M. Sayeed

Electrical and Computer Engineering
University of Wisconsin-Madison
akbar@engr.wisc.edu

ABSTRACT

Most existing works in wireless communications assume rich multipath. In particular, the intense research on multi-antenna (MIMO) systems in the last decade was pioneered by results based on an i.i.d. channel model representing a rich multipath environment. However, there is growing experimental evidence that physical wireless channels exhibit a sparse multipath structure, especially at large bandwidths. In this paper, we propose a model for sparse multipath channels and discuss its implications for channel learning and optimal communication. Our investigation is based on a virtual representation of physical wireless channels that corresponds to uniform sampling of the scattering environment in angle-delay-Doppler at a resolution commensurate with the signal space dimensions. The virtual representation characterizes the statistically independent degrees of freedom (DoF) in the channel and a key implication of sparse multipath is that the DoF scale sub-linearly with the signal space dimensions in contrast to the linear scaling inherent in rich multipath. We first show that sparse multipath channels are perfectly learnable (and hence coherent) in the limit of large bandwidth. We next study the potential of reconfigurable arrays in maximizing MIMO capacity in sparse multipath. Simulation results are presented to illustrate the capacity gains.

1. INTRODUCTION

Multipath signal propagation, the most salient feature of wireless channels, is a curse and a blessing from the viewpoint of capacity and reliability of such channels. On the one hand, multipath leads to signal fading – fluctuations in received signal strength – that severely impacts the reliability of such channels. On the other hand, knowledge of multipath structure can be exploited for diversity – multiple independent modes of communication – to increase the rate and/or reliability of communication. The impact of fading versus diversity on performance is governed by the the amount of channel state information (CSI) known to the system. For example, if perfect CSI is available at the receiver (coherent communication), then the reliablity of the fading channel converges to that of the AWGN as the level of diversity increases. Furthermore, the gap in the performance of coherent or non-coherent communication is generally quite significant.

Technological advances in wideband multi-antenna RF front-ends are enabling learning CSI at a finer resolution afforded by the increase in the spatio-temporal signal space dimensions. Accurate modeling of channel characteristics in time, frequency and space, as a function of physical multipath characteristics, is thus critical for analyzing the impact of such emerging sophisticated RF front ends. In particular, while most existing models for wirless channels assume a rich multipath environment, there is growing experimental evidence that physical channel exhibit a sparse structure even with small number of antennas and especially at wide bandwidths (see, e.g., [1]). In this paper, we use a virtual representation of physical multipath channels that we have developed in the past several years to present a framework for modeling spare multipath channels and to study certain the implications of sparsity on channel learning and optimal communication. The virtual representation samples the multipath geometry in angle-delay-Doppler at a resolution commensurate with the signal space dimensions and characterizes the statistically independent degrees of freedom (DoF) available for communication. Sparse channels correspond to a sparse set of dominant non-vanishing virtual coefficients. A key implication of sparse multipath is that the DoF scale sub-linearly with the signal space dimensions in contrast to the linear scaling inherent in most existing models that implicitly assume a rich multipath. Sparsity of multipath in angle-delay-Doppler leads to channel coherence in time, frequency and space that has significant implications for optimal communication in the low-SNR/wideband regime. In particular, we show that sparse multipath channels are perfectly learnable in the limit of large bandwidth and thus naturally bridge the gap between coherent and non-coherent extremens. From a spatial viewpoint, we argue that adapting the array configurations (antenna spacings) can dramatically increase MIMO capacity in sparse multipath in the low-SNR regime. Our results indicate that, surprisingly, three canonical array configurations are sufficient for near-optimum performance over all SNR's. Simulation results are presented to illustrate the capacity gains due to reconfigurable arrays.

2. VIRTUAL MODELING OF PHYSICAL WIRELESS CHANNELS

Consider a time- and frequency-selective multi-antenna (MIMO) channel corresponding to a transmitter with N_T antennas and a receiver with N_R antennas. For simplicity, we assume uniform linear arrays (ULA's) of antennas and consider signaling over this channel over a duration T and (two-sided) bandwidth W. In the absence of noise, the transmitted and received signal are related as

$$\mathbf{x}(t) = \int_{-W/2}^{W/2} \mathbf{H}(t,f)\mathbf{S}(f)e^{j2\pi ft}df \ , \ 0 \leq t \leq T \qquad (1)$$

where $\mathbf{x}(t)$ is the N_R-dimensional received signal, $\mathbf{S}(f)$ is the Fourier transform of the N_T-dimensional transmitted signal $\mathbf{s}(t)$, and $\mathbf{H}(t,f)$ if the $N_R \times N_T$ time-varying frequency response matrix of the channel. A physical wireless channel can be accurately modeled as

$$\mathbf{H}(t,f) = \sum_{n=1}^{N_{path}} \beta_n \mathbf{a}_R(\theta_{R,n})\mathbf{a}_T^H(\theta_{T,n})e^{j2\pi\nu_n t}e^{-j2\pi\tau_n f} \qquad (2)$$

which represents signal propagation over N_{path} paths; β_n denotes the complex path gain, $\theta_{R,n}$ the angle of arrival (AoA), $\theta_{T,n}$ the

This work was partly supported by NSF under grant CCF-0431088.

angle of departure (AoD), τ_n the delay and ν_n the Doppler shift associated with the n-th path. The vectors $\mathbf{a}_T(\theta_T)$ and $\mathbf{a}_R(\theta_R)$ denote the array steering and response vectors for transmitting/receiving a signal in the direction θ_T/θ_R and are periodic in θ with unit period [8].[1] We assume that $\tau_n \in [0, \tau_{max}]$ and $\nu_n \in [-\frac{\nu_{max}}{2}, \frac{\nu_{max}}{2}]$ where τ_{max} denotes the delay spread and ν_{max} the (two-sided) Doppler spread of the channel. We also assume maximum angular spreads, $(\theta_{R,n}, \theta_{T,n}) \in [-1/2, 1/2] \times [-1/2, 1/2]$, at critical ($d = \lambda/2$) antenna spacing. Finally, we assume that over the timescales of interest, $\{\theta_{T,n}, \theta_{R,n}, \tau_n, \nu_n\}$ remain fixed; the only variation in the channel is due to variations in amplitude and phases of $\{\beta_n\}$ which are independent across paths.

While accurate (non-linear) estimation of AoA's, AoD's, delays and Doppler shifts is critical in radar *imaging* applications, it is not critical in a communications context since the ultimate goal is to reliably communicate information over the channel. Studying the key communication-theoretic characteristics of time-varying, wideband MIMO channels is greatly facilitated by a *virtual representation* of the physical model (2) that we have developed in the past several years [8, 9]

$$\mathbf{H}(t,f) \approx \sum_{i=1}^{N_r}\sum_{k=1}^{N_t}\sum_{\ell=0}^{L}\sum_{m=-M}^{M} H_v(i,k,\ell,m) \mathbf{a}_R\left(\frac{i}{N_r}\right)\mathbf{a}_T^H\left(\frac{k}{N_t}\right)e^{j2\pi\frac{m}{T}t}e^{-j2\pi\frac{\ell}{W}f} . \quad (3)$$

Comparing (2) and (3), we note that the virtual representation corresponds to sampling the physical angle-delay-Doppler space at uniformly spaced virtual AoA's, AoD's, delays and Doppler shifts at a resolution commensurate with the signal space parameters: $\Delta\theta_R = 1/N_R$, $\Delta\theta_T = 1/N_T$, $\Delta\tau = 1/W$, $\Delta\nu = 1/T$. In (3), $L = \lceil W\tau_{max}\rceil$ denotes the maximum number of resolvable delays and $M = \lceil T\nu_{max}/2\rceil$ the maximum number of resolvable Doppler shifts. For maximum angular spreads, N_T and N_R reflect the maximum number of resolvable AoD's and AoA's. Note that due to the fixed angle-delay-Doppler sampling, the virtual representation is a *linear* channel representation and is characterized by the virtual channel coefficients $\{H_v(i,k,\ell,m)\}$.

2.1. Virtual Path Partitioning

A key property of the virtual representation is that its coefficients partition the propagation paths into approximately disjoint subsets. Specifically, define the following subsets of paths based on their resolution in angle, delay and Doppler

$$\begin{aligned} S_{R,i} &= \{n : \theta_{R,n} \in i/N_R + (-1/2N_R, 1/2N_R]\} \\ S_{T,k} &= \{n : \theta_{T,n} \in k/N_T + (-1/2N_T, 1/2N_T]\} \\ S_{\tau,\ell} &= \{n : \tau_n \in \ell/W + (-1/2W, 1/2W]\} \\ S_{\nu,m} &= \{n : \nu_n \in m/T + (-1/2T, 1/2T]\} . \end{aligned} \quad (4)$$

It can be shown that [8, 9]

$$H_v(i,k,\ell,m) \approx \sum_{n\in S_{R,i}\cap S_{T,k}\cap S_{\tau,\ell}\cap S_{\nu,m}} \beta_n \quad (5)$$

where a phase and attentuation factor has been absorbed in β_n. The relation (5) states that each $H_v(i,k,\ell,m)$ is approximately equal to the sum of the gains of all physical paths whose angles, delays and Doppler shifts lie within an *angle-delay-Doppler resolution bin* of size $\Delta\theta_R \times \Delta\theta_T \times \Delta\tau \times \Delta\nu$ centered around $(i/N_R, k/N_T, \ell/W, m/T)$ in the $(\theta_R, \theta_T, \tau, \nu)$ space. It follows that *distinct* $H_v(i,k,\ell,m)$'s correspond to approximately[2] *disjoint* subsets of paths and are hence the virtual channel coefficients are approximately statistically independent (due to independent path gains and phases). We assume that the virtual coefficients are perfectly independent. Thus, for Rayleigh fading, the channel statistics are characterized by the power in the virtual coefficients

$$\begin{aligned} \Psi(i,k,\ell,m) &= E[|H_v(i,k,\ell,m)|^2] \\ &\approx \sum_{n\in S_{R,i}\cap S_{T,k}\cap S_{\tau,\ell}\cap S_{\nu,m}} E[|\beta_n|^2] . \end{aligned} \quad (6)$$

which is a measure of the angle-delay-Doppler power spectrum.

2.2. Degrees of Freedom

The number of dominant non-vanishing[3] $\{H_v(i,k,\ell,m)\}$, represent the statistically independent *degrees of freedom (DoF)*, D, in the channel that govern its capacity and diversity. The maximum number of DoF is given by

$$D \le D_{max} = N_R N_T (L+1)(2M+1) \approx N_R N_T T W \tau_{max}\nu_{max} \quad (7)$$

which corresponds to the maximum number of *resolvable* paths within the angular, delay and Doppler spreads. By virtue of (5), we have $D_{max} \le N_{path}$; $D = D_{max}$ if there are at least $N_{path} \ge D_{max}$ *resolvable* paths so that each angle-delay-Doppler resolution bin is populated by a path.

3. SPARSE MULTIPATH WIRELESS CHANNELS

Let $N_s = N_R N_T T W$ denote the number of spatio-temporal signal space dimensions. From (7) we note that for underspread channels ($\tau_{max}\nu_{max} < 1$), $D_{max} < N_s$. All existing models for wideband MIMO channels are implicitly based on the wide-sense stationary uncorrelated scattering (WSSUS) assumption which in turn implies a *rich scattering* environment in which there are sufficiently many paths so that the channel DoF scale *linearly* with the signal space dimensions

$$D_{rich} = D_{max} = O(N_s) = cN_s \ , \ 0 < c < 1 . \quad (8)$$

In physical channel encountered in practice, the number of paths may not be large enough to excite D_{max} DoF, especially as we increase the signal space dimensions by increasing the number of antennas, bandwidth, or signaling duration. This has been supported by experimental measurement campaigns, both for indoor MIMO channels, and ultrawideband single-antenna channels (see, e.g., [1]). When $D < D_{max}$, we refer to such channels as *sparse multipath* channels. The focus of this paper is to develop a modeling framework for sparse multipath channels and to study the implications of sparse multipath on fundamental limits of performance. We formalize this notion of sparsity in the following definition.

[1] The normalized angle variable θ is related to the physical angle ϕ (measured with respect to array broadside) as $\theta = d\sin(\phi)/\lambda$ where d is the antenna spacing and λ is the wavelength of propagation.

[2] Due to the sidelobes associated with finite signal space dimensions.

[3] For which $\Psi(i,k,\ell,m) > \epsilon > 0$ for some chosen ϵ.

Definition 1 (Spare Multipath Channels)**.** *Let D denote the number of dominant non-vanishing virtual channel coefficients, representing the statistically independent DoF in the channel: $D = |\{(i,k,\ell,m) : |H_v(i,k,\ell,m)| > \epsilon\}|$ for some appropriately chosen $\epsilon > 0$. A sparse multipath channel satisfies $D < D_{max}$ and furthermore the channel DoF scale* sub-linearly *with the signal space dimensions*

$$D = o(N_s) \longleftrightarrow \lim_{N_s \to \infty} \frac{D}{N_s} = 0 \tag{9}$$

Remark 1. *The value of ϵ in general depends on the operating SNR. For simplicity, in this paper we assume that the D dominant virtual coefficients have a constant variance, and the rest of the coefficients are identically zero. Specifically, we focus on channels with sub-linear DoF scaling of the form*

$$\begin{aligned} D &= D_{S,max}^{\gamma} D_{T,max}^{\delta_1} D_{W,max}^{\delta_2} \\ &= (N_T N_R)^{\gamma} (T\nu_{max})^{\delta_1} (W\tau_{max})^{\delta_2} , \end{aligned} \tag{10}$$

for some $\gamma, \delta_1, \delta_2 \in [0,1]$, where $D_{S,max} = N_T N_R$, $D_{T,max} = T\nu_{max}$ and $D_{W,max} = W\tau_{max}$ denote the maximum number of DoF in the spatial, temporal and spectral dimensions, respectively. The extreme case $\gamma = \delta_1 = \delta_2 = 1$ represents a rich multipath environment in which D scales linearly with N_s. On the the other extreme, $\gamma = \delta_1 = \delta_2 = 0$ represents a very sparse environment with a fixed number of paths in which D remains constant regardless of N_s.

Sparse multipath channels represent a sparse distribution of *resolvable* paths in the angle-delay-Doppler space. Sparsity in angle-delay-Doppler leads to the notion of *coherence* in space-frequency-time due to the Fourier duality between angle-delay-Doppler and space-frequency-time. In the rest of the paper we explore the implications of sparsity/coherence for communication in the wideband/low-power regime. In Sec. 4, we discuss the implications of sparsity for single-antenna time-varying wideband channels. In Sec. 5, we discuss the impact of reconfigurable arrays on the capacity of sparse narrowband MIMO channels.

4. SPARSITY IN DELAY-DOPPLER

In the single antenna case the physical model (2) and the virtual representation (3) reduce to

$$H(t,f) = \sum_n \beta_n e^{j2\pi\nu_n t} e^{-j2\pi\tau_n f} \tag{11}$$

$$\approx \sum_{\ell=0}^{L} \sum_{m=-M}^{M} H_v(\ell,m) e^{j2\pi\frac{m}{T}t} e^{-j2\pi\frac{\ell}{W}f} \tag{12}$$

$$H_v(\ell,m) \approx \sum_{n \in S_{\tau,\ell} \cap S_{\nu,m}} \beta_n \tag{13}$$

and the signal at the receiver is represented as

$$x(t) = \sum_n \beta_n e^{j2\pi\nu_n t} s(t-\tau_n) + w(t) \tag{14}$$

$$\approx \sum_{\ell} \sum_{m} H_v(\ell,m) e^{j2\pi\frac{m}{T}} s(t-\ell/W) + w(t) \tag{15}$$

where $w(t)$ denote the AWGN at the receiver. The virtual coefficients $\{H_v(\ell,m)\}$ sample the scattering environment in delay-Doppler at resolutions $\Delta\tau = 1/W$ and $\Delta\nu = 1/T$, as illustrated in Fig.1(a). Each square in the figure represents an angle-delay resolution bin corresponding to a particular $H_v(\ell,m)$ and the dotted resolution bins represent the dominant non-vanishing virtual coefficients (DoF). The DoF in this case represent the *delay-Doppler diversity* afforded by the channel [10]. The delay-Doppler DoF

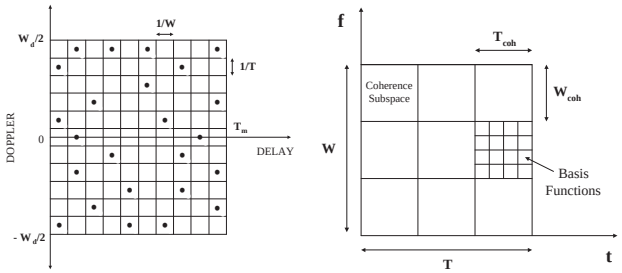

(a) (b)

Figure 1: *(a) Delay-doppler sampling commensurate with T and W. ($T_m = \tau_{max}$ and $W_d = \nu_{max}$.) (b) Time-frequency coherence subspaces in short-time Fourier signaling.*

satisfy

$$\begin{aligned} D &= D_T D_W \le D_{max} = D_{T,max} D_{W,max} \\ D_T &\sim D_{T,max}^{\delta_1} , \; D_W \sim D_{W,max}^{\delta_2} , \; \delta_1, \delta_2 \in [0,1] \end{aligned} \tag{16}$$

$D_{T,max}$ and $D_{W,max}$ are defined in (10) and denote the maximum number of resolvable Doppler shifts and delays, respectively. Rich multipath corresponds to $\delta_1 = \delta_2 = 1$ in which $D = D_{max} = O(N_s) = O(TW)$ and both $D_{T,max}$ and $D_{W,max}$ scale linearly with T and W, respectively; each delay-Doppler resolution bin in Fig. 1(a) is populated with a path. On the other hand, physical multipath channels correspond to $\delta_1, \delta_2 < 1$, in which $D = o(N_s)$ as illustrated by the dotted resolution bins in Fig. 1(a), and get sparser with increasing W due to fewer than $D_{W,max}$ resolvable delays and with increasing T due to fewer than $D_{T,max}$ resolvable Doppler shifts. The smaller the value of δ_i, the slower the growth in the corresponding domain.

4.1. Time-Frequency Coherence

Signaling over orthogonal short-time Fourier (STF) (or Gabor) basis functions provides a very attractive approach for communication over rapidly time-varying multipath channels since appropriately chosen STF basis functions serve as approximate eigenfunctions for underspread channels [4, 3]. Representing (14) with respect to the STF basis yields an $N_s = TW$-dimensional matrix system equation $\mathbf{x} = \mathbf{H}\mathbf{s} + \mathbf{w}$ where $\mathbf{s}$, $\mathbf{x}$ and $\mathbf{w}$ represent the projections of $s(t)$, $x(t)$ and $w(t)$ onto the (orthonormal) STF basis [4]. The $N_s \times N_s$ matrix $\mathbf{H}$ is a representation of the channel in the STF domain and is *approximately diagonal* due to the approximate eigen-property of STF basis functions. We assume $\mathbf{H}$ to be exactly diagonal. Delay-Doppler diversity leads to the notion of *time-frequency coherence subspaces* in the STF domain [4], illustrated in Fig. 1(b), which is captured by an intuitive block fading representation for $\mathbf{H}$:

$$\mathbf{H} = \mathrm{diag}\Big[\underbrace{h_{1,1} \cdots h_{1,N_c}}_{\text{Subspace 1}}, \; \underbrace{h_{2,1} \cdots h_{2,N_c}}_{\text{Subspace 2}} \; \cdots \; \underbrace{h_{D,1} \cdots h_{D,N_c}}_{\text{Subspace } D} \Big] . \tag{17}$$

As illustrated in Fig. 1(b), the signal space is partitioned into D statistically independent *coherence subspaces*, $N_s = TW = N_c D$, where D represents the DoF (delay-Doppler diversity) and N_c represents the dimension of each coherence subspace. In the block fading model (17), the channel coefficients over the i-th coherence subspace are assumed to be identical (perfectly correlated), $h_i = h_{i,1} = \cdots h_{i,N_c}$, and the channel coefficients over different coherence subspaces are assumed to be i.i.d. complex Gaussian random variables $\mathcal{CN}(0,1)$. The coherence dimension is given by

$$N_c = T_{coh} W_{coh} = \frac{TW}{D_T D_W} = \frac{T^{1-\delta_1}}{\nu_{max}^{\delta_1}} \frac{W^{1-\delta_2}}{\tau_{max}^{\delta_2}} \geq \left\lceil \frac{1}{\tau_{max}\nu_{max}} \right\rceil \tag{18}$$

where $T_{coh} = T^{1-\delta_1}/\nu_{max}^{\delta_1}$ is the *coherence time* and $W_{coh} = W^{1-\delta_2}/\tau_{max}^{\delta_2}$ is the *coherence bandwidth* of the channel. In the following, we assume $\delta_1 = \delta_2 = \delta$ for simplicity. Note that $\delta = 1$ corresponds to rich multipath in which N_c is fixed and $D = D_{max}$ increases linearly with $N_s = TW$. In the other extreme of $\delta = 0$, D is fixed and N_c scales linearly with N_s. For $\delta \in (0,1)$, both N_c and D *increase sub-linearly* with $N_s = TW$.

4.2. Asymptotic Coherence of Sparse Channels

Sparsity in delay-Doppler leads to a fundamental *diversity versus learnability tradeoff* in communication over time-varying multipath channels. With perfect channel state information (CSI) at the receiver (coherent communication), D, represents the level of diversity afforded by the channel to enhance reliability against fading. On the other hand, if the channel is unknown at the receiver (non-coherent communication), D reflects the level of uncertainty in the channel. It is well-known that the capacity of an ergodic multipath channel approaches the AWGN capacity in the limit of large bandwidth; however, the rate of convergence is much slower in the non-coherent case compared to the coherent case. Recent results have shown that coherence in time-frequency can bridge the gap between the coherent and non-coherent regimes by explicitly or implicitly estimating the D channel parameters [11, 5]. As we argue next, the gap between coherent and non-coherent regimes vanishes asymptotically (large T, W) for sparse multipath channels. Thus, we say that sparse multipath channels are *asymptotically coherent*. We demonstrate this by analyzing the performance of a simple training-based communication scheme.

The training scheme described here is similar to the one in [11], adapted to the STF framework [5]. Let P denote the average transmit power. The total energy available for training and communication over the duration T is PT of which a fraction η is used for training and the remaining fraction $(1-\eta)$ is used for communication. We use the mean square error (MSE) of the estimated channel coefficients, h_i , $i = 1, \cdots, D$, as a measure of the quality of estimation. Under the block fading model, the scheme uses one STF dimension in each coherence subspace for training and the remaining $(N_c - 1)$ dimensions for communication. For a given η, the training energy per coherence subspace and the MSE associated with the minimum mean squared error (MMSE) estimate of each h_i are given by

$$E_{tr} = \frac{\eta TP}{D} = \eta N_c \mathsf{SNR} \ , \ \mathrm{MSE} = E\left[|h_i - \widehat{h}_i|^2\right] = \frac{1}{1+E_{tr}} \tag{19}$$

where $\mathsf{SNR} = \frac{P}{W}$ which goes to zero as $W \to \infty$.

The performance of channel estimation is measured using: (i) MSE of channel estimates and (ii) optimal fraction of energy used for estimation, η^*. It can be shown that η^*, from the viewpoint of maximizing capacity [5] or maximizing reliability (error exponent) [2], is given by

$$\eta^* = \frac{N_c\mathsf{SNR} + N_c - 1}{(N_c-2)N_c\mathsf{SNR}} \left[\sqrt{1 + \frac{(N_c-2)N_c\mathsf{SNR}}{N_c\mathsf{SNR} + N_c - 1}} - 1 \right] \tag{20}$$

The following result formalizes the asymptotic coherence of sparse channels [2].

Theorem 1. *In the limit of large signal space dimensions ($T, W \to \infty$, $\mathsf{SNR} \to 0$)*

$$\mathrm{MSE} = \frac{1}{1+\eta^* \mathrm{N_c} \mathsf{SNR}} \to 0 \quad \textit{and} \quad \eta^* \to 0 \tag{21}$$

if and only if $N_c \sim \frac{1}{\mathsf{SNR}^\mu}$, for $\mu > 1$.

The above results states that a time- and frequency-selective multipath channel is asymptotically coherent – perfectly learnable with a vanishing fraction of energy expended on training – if and only if N_c scales with SNR at the specified rate. This condition is not satisfied for rich channels ($\delta = 1$) since N_c is constant. In fact, in this case, $\eta^* \to \frac{1}{2}$ in (20), $E_{tr} \to 0$ and, hence, $\mathrm{MSE} \to 1$.

On the other hand, the N_c condition in Thm. 1 is *always* satisfied for sparse channels, if T scales with W at an appropriate rate. From (18) we have $N_c = \frac{(TW)^{1-\delta}}{(\tau_{max}\nu_{max})^\delta}$. Substuting $T = W^\alpha$ for some $\alpha > 0$ and $\mathsf{SNR} = \frac{P}{W}$ in this relation leads to $N_c \sim \frac{1}{\mathsf{SNR}^{(1+\alpha)(1-\delta)}}$. Thus, we need $\mu = (1+\alpha)(1-\delta) > 1 \longleftrightarrow \alpha > \frac{\delta}{(1-\delta)}$ for the asymptotic coherence condition to hold, which can be satisfied for $\delta \in (0,1)$. The (qualitative[4]) scaling behavior of MSE and η^* as a function of W is illustrated in Fig. 2 for three different values of μ. Note that asymptotic coherence is only achieved for $\mu > 1$; the underlying required value of α for T-W scaling can be inferred as $\alpha = \mu/(1-\delta) - 1$.

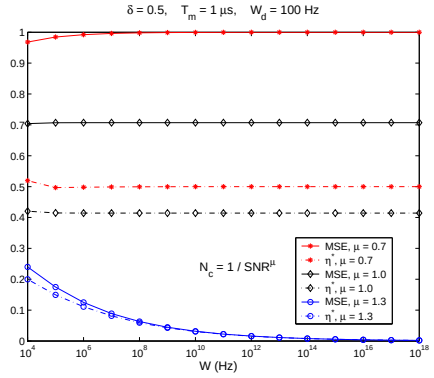

Figure 2: *MSE and η^* as a function of W for three different coherence scaling laws.*

[4]Since we are ignoring scaling constants.

5. SPARSITY IN THE SPATIAL DOMAIN

For narrowband MIMO channels, the physical and virtual models reduce to

$$\mathbf{H} = \sum_{n=1}^{N_{path}} \beta_n \mathbf{a}_R(\theta_{R,n}) \mathbf{a}_T^H(\theta_{T,n}) \quad (22)$$

$$= \sum_{i=1}^{N_r} \sum_{k=1}^{N_t} H_v(i,k) \mathbf{a}_R\left(\frac{i}{N_r}\right) \mathbf{a}_T^H\left(\frac{k}{N_t}\right) \quad (23)$$

$$H(i,k) \approx \sum_{n \in S_{R,i} \cap S_{T,k}} \beta_n \quad (24)$$

The statistics of $\mathbf{H}$ are characterized by the virtual channel power matrix $\mathbf{\Psi}$: $\mathbf{\Psi}(i,k) = E[|\mathbf{H}_v(i,k)|^2]$. For simplicity, consider $N = N_T = N_R$. For sparse MIMO channels, $D < D_{max} = N^2$, as illustrated in Fig. 3(a). In [7] we revisited coherent capacity *scaling* in MIMO channels with N and argued that the DoF (and channel power) can at best scale at a *sub-quadratic* rate, $D(N) = o(N^2)$, and consequently the capacity of physical channels can at best scale at a *sub-linear* rate which cannot exceed $\mathcal{O}\left(\sqrt{D(N)}\right) = o(N)$. We also introduced the notion of an ideal MIMO channel that achieves $\mathcal{O}\left(\sqrt{D(N)}\right)$ capacity scaling.

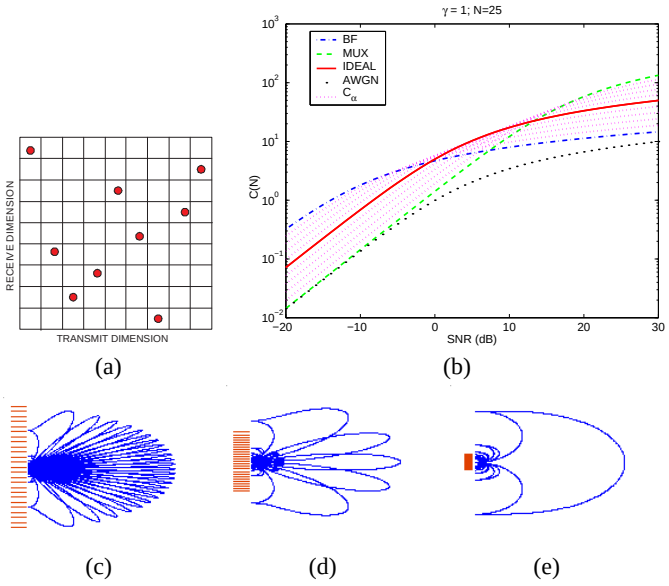

Figure 3: (a) A sparse 9 x 9 virtual channel matrix. (b) Capacity versus SNR for different channel configurations for D=N=25. (c)-(e): Virtual beam directions for $N = 25$ and different spacings; (c) large spacing; (d) medium spacing; (e) small spacing.

A sparse $\mathbf{H}_v$ provides a model for spatial correlation in $\mathbf{H}$: in general, the sparser the $\mathbf{H}_v$, the higher the correlation in $\mathbf{H}$. For simplicity, assume that the D non-vanishing entries are $\mathcal{CN}(0,1)$. It is convenient to model a sparse $\mathbf{H}_v$ as

$$\mathbf{H}_v = \mathbf{M} \odot \mathbf{H}_{iid} \quad (25)$$

where $\odot$ denotes element-wise product, $\mathbf{H}_{iid}$ is an i.i.d. matrix with $\mathcal{CN}(0,1)$ entries, and $\mathbf{M}$ is a mask matrix with D unit entries and zeros elsewhere. Under these assumptions, $\mathbf{\Psi} = \mathbf{M}$.

The ergodic capacity of a MIMO channel, assuming knowledge of $\mathbf{H}$ at the receiver, is given by

$$C(N,\rho) = \max_{\mathrm{Tr}(\mathbf{Q}) \le \rho} E_{\mathbf{H}_v}\left[\log\det\left(\mathbf{I} + \mathbf{H}_v \mathbf{Q} \mathbf{H}_v^H\right)\right] \quad (26)$$

where ρ is the transmit SNR, and $\mathbf{Q} = E[\mathbf{s}_v \mathbf{s}_v^H]$ is the transmit covariance matrix in beamspace. It has been shown that the capacity-maximizing $\mathbf{Q}_{opt}$ is diagonal. Furthermore, for general correlated channels, $\mathbf{Q}_{opt}$ is full-rank at high SNR's, whereas it is rank-1 (beamforming) at low SNR's. As ρ is increased from low to high SNR's, the rank of $\mathbf{Q}_{opt}$ increases from 1 to N.

5.1. The Ideal MIMO Channel

The capacity of a sparse virtual channel matrix $\mathbf{H}_v$ depends on three fundamental quantities: 1) the transmit SNR ρ, 2) the number of DoF, $D < N^2$, and 3) the distribution of the D DoF in the available N^2 dimensions. We showed in [7] that for any ρ, there is an optimal mask matrix $\mathbf{M}_{opt}$ that yields the highest capacity at that ρ. We term the corresponding MIMO channel the Ideal MIMO Channel at that ρ.

Definition 2 (Ideal MIMO Channel)**.** *Consider a fixed N and $D < N^2$ and let $\mathcal{M}(D)$ denote the set of all $N \times N$ mask matrices with D non-zero (unit) entries. For any ρ, the ideal MIMO capacity is defined as*

$$C_{id}(N,D,\rho) = \max_{\mathbf{M} \in \mathcal{M}(D)} C(N,\rho,\mathbf{M}) \quad (27)$$

and an $\mathbf{M}_{opt}$ that achieves $C_{id}(N,D,\rho)$ defines the Ideal MIMO Channel at that ρ. □

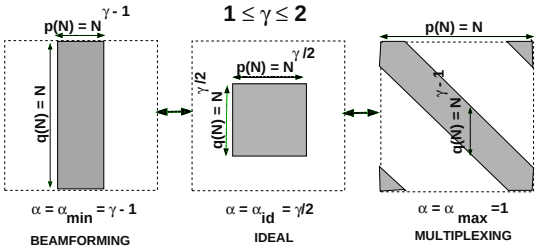

Figure 4: A family of mask matrices. $\gamma \in [1,2]$.

In [7] we presented an explicit family of mask matrices to characterize a particular $\mathbf{M}_{opt}$ for any given ρ. The family of mask matrices is defined by two parameters (p,q) such that $D = pq$. For $D = N^\gamma$, $\gamma \in [0,2]$, the matrices can be further parameterized via $p = N^\alpha$, $\alpha \in [\alpha_{min}, \alpha_{max}]$ where $\alpha_{min} = \max(\gamma - 1, 0)$ and $\alpha_{max} = \min(\gamma, 1)$, and $q = D/p$. For a given p, the mask matrix $\mathbf{M}(D,p)$ is an $N \times N$ matrix but its non-zero entries are contained in a non-zero sub-matrix of size $r \times p$, $r = \max(q,p)$, consisting of p non-zero columns, and q non-zero (unit) entries in each column. The mask matrices are illustrated in Fig. 4 for $\gamma \in [1,2]$.

The following theorem, which can be inferred form the results in [7], characterizes the Ideal MIMO Channel at any ρ.

Theorem 2. *For sufficiently large N, the capacity of the MIMO channel defined by a mask $\mathbf{M}(D,p)$ is accurately approximated as a function of ρ by*

$$C(N,\rho,\mathbf{M}(D,p)) \approx p \log\left(1 + \rho \frac{D}{p^2}\right) \quad (28)$$

For a given ρ, the Ideal MIMO Channel is characterized by $\mathbf{M}(D, p_{opt})$ p_{opt} where

$$p_{opt} \approx \begin{cases} p_{min} & , \quad \rho < \rho_{low} \\ \frac{\sqrt{\rho D}}{2} & , \quad \rho \in [\rho_{low}, \rho_{high}] \\ p_{max} & , \quad \rho > \rho_{high} \end{cases} \tag{29}$$

and $C_{id}(N, D, \rho) = C(N, \rho, \mathbf{M}(D, p_{opt}))$. In (29), $p_{min} = N^{\alpha_{min}}$, $p_{max} = N^{\alpha_{max}}$, $\rho_{low} \approx 4p_{min}^2/D = 4N^{2\alpha_{min}}/D$ and $\rho_{high} \approx 4p_{max}^2/D = 4N^{2\alpha_{max}}/D$. □

Remark 2. ***Three Canonical Array Configurations****. Three canonical channel configurations are highlighted in Fig. 3 corresponding to $N = D = 25$: BF: $\mathbf{H}_{v,bf} \leftrightarrow p_{bf} = p_{min} = 1$; IDEAL: $\mathbf{H}_{v,id} \leftrightarrow p_{id} = \sqrt{D} = \sqrt{N}$; and MUX: $\mathbf{H}_{v,mux} \leftrightarrow p_{mux} = p_{max} = N$. The BF and MUX configurations represent the Ideal MIMO Channel for $\rho < \rho_{low}$ and $\rho > \rho_{high}$, respectively. As evident from the figure, the IDEAL configuration (optimal from a capacity scaling viewpiont) is a good approximation to the Ideal MIMO Channel for $\rho \in (\rho_{low}, \rho_{high})$. Thus, from a practical viewpoint, these three configurations suffice for adapting array configurations to maximize capacity over the entire SNR range.*

5.2. Creating the Ideal MIMO Channel with Reconfigurable Arrays

We present a numerical example to illustrate the creation of the three canonical channel configurations, $\mathbf{H}_{v,mux}$, $\mathbf{H}_{v,id}$, and $\mathbf{H}_{v,bf}$, by adapting the antenna spacings at the transmitter (d_t) and receiver (d_r) as illustrated in Fig. 3(c)-(e). We consider $N = D = 25$ ($\gamma = 1$) and first generate the AoA's and AoD's $(\theta_{r,n}, \theta_{t,n}) \in [-1/2, 1/2]^2$ for $N_{path} = 25$ paths, where the AoA/AoD's of different paths are randomly distributed over the entire angular spread. This defines $\mathbf{H}_{mux}$ environment for $d_{t,mux} = d_{r,mux} = d_{max} \geq \lambda/2$ (Fig. 3(c)). These AoA/AoD's are then fixed and the capacities of the different configurations are estimated via 200 channel realizations, simulated using (22) by independently generating $\mathcal{CN}(0, 1)$ complex path gains. The random locations of the D paths are illustrated in Fig. 5(a), which shows the contour plot of $\mathbf{\Psi}_{mux}$. The spacings for $\mathbf{H}_{v,bf}$ are $d_{t,bf} = d_{t,mux}/N$ (Fig. 3(e)) and $d_{r,bf} = d_{r,mux}$ (Fig. 3(c)), whereas the spacings for $\mathbf{H}_{id}$ are $d_{t,id} = d_{r,id} = d_{r,mux}/\sqrt{N}$ (Fig. 3(d)). The contour plots of the resulting $\mathbf{\Psi}_{id}$ and $\mathbf{\Psi}_{bf}$ are shown in Figs. 5(b) and (c) (compare with Fig. 4). The numerically estimated capacities for the three configurations are plotted in Fig. 5(d) along with the theoretical curves in Fig. 3(b) using (28). (see [6] for more details.)

Remark 3 (Physical Source-Channel Matching)**.** *The capacity maximizing input for fixed spacings (see (26)) allocates all power to the strongest virtual direction at low ρ. With reconfigurable arrays, d_t is decreased with ρ to concentrate channel power in fewer non-vanishing virtual transmit dimensions. This reflects a form of source-channel matching: the rank of the optimal input is better-matched to the rank of $\mathbf{H}_v$. Physically, as d_t is decreased, fewer data streams (p) are transmitted over a corresponding number of spatial beams, whereas the width of the beams gets wider.*

6. REFERENCES

[1] S. Ghassemzadeh, R. Jana, C. Rice, W. Turin, and V. Tarokh. Measurement and modeling of an ultra-wide bandwidth indoor channel. Communication Theory Workshop, May 2002.

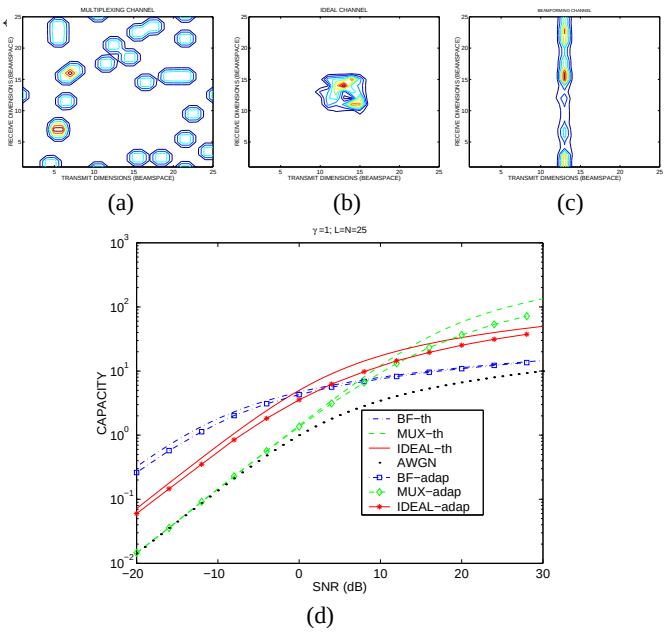

Figure 5: (a)-(c): Contour plots of $\mathbf{\Psi}$ for the three canonical configurations in an environment with N=D=25 randomly distributed paths; (a) $\mathbf{\Psi}_{mux}$; (b) $\mathbf{\Psi}_{id}$; (c) $\mathbf{\Psi}_{bf}$. (d) The numerical capacities of the three configurations, along with the theoretical values.

[2] G. Hariharan and A. Sayeed. Reliability of sparse wideband channels. *in preparation*.

[3] W. Kozek and A. F. Molisch. Nonorthogonal pulseshapes for multicarrier communications in doubly dispersive channels. *IEEE J Select. Areas Commun.*, pp. 1579–1589, Oct. 1998.

[4] K. Liu, T. Kadous, and A. M. Sayeed. Orthogonal time-frequency signaling for doubly dispersive channels. *IEEE Trans. Inform. Th.*, pp. 2583–2603, Nov. 2004.

[5] V. Raghavan, G. Hariharan, and A. Sayeed. Exploiting time-frequency coherence to achieve coherent capacity in wideband wireless channels. In *Proc. 43rd Annual Allerton Conference*, Sep. 2005.

[6] A. Sayeed and V. Raghavan. The ideal MIMO channel: Maximizing capacity in sparse multipath with reconfigurable antenna arrays. *to be presented at the IEEE Intl. Symp. Inform. Th.*, July 2006.

[7] A. Sayeed, V. Raghavan, and J. Kotecha. Capacity of space-time wireless channels: A physical perspective. In *2004 Proc. Information Theory Workshop*, Sep. 2004.

[8] A. M. Sayeed. Deconstructing multi-antenna fading channels. *IEEE Trans. Signal Processing*, pp. 2563–2579, Oct. 2002.

[9] A. M. Sayeed. A virtual representation for time- and frequency-selective correlated MIMO channels. *Proc. ICASSP 2003*, 4:648–651, 2003.

[10] A. M. Sayeed and B. Aazhang. Joint multipath-Doppler diversity in mobile wireless communications. *IEEE Trans. Commun.*, pp. 123–132, Jan. 1999.

[11] L. Zheng, M. Medard, and D. Tse. Channel coherence in the low snr regime. In *41-st Annual Allerton Conference*, Oct. 2003.